Int. J. Heat Mass Transfer. Vol. 34, No. 8, pp. 2071–2079, 1991
Printed in Great Britain

0017–9310/91 $3.00+0.00
Pergamon Press plc

Pool boiling heat transfer on finned tubes—an experimental and theoretical study

E. HAHNE, CHEN QIU-RONG and R. WINDISCH
Institut für Thermodynamik und Wärmetechnik, Universität Stuttgart, Pfaffenwaldring 6, D-7000 Stuttgart 80, F.R.G.

(*Received* 16 *March* 1990)

Abstract—Pool boiling heat transfer of R11 is investigated experimentally and theoretically on single tubes and twin tube arrangements. Finned tubes with 19 and 26 fins per inch (fpi) are used. The refrigerant evaporates at a saturation state of 1 bar on the outside of the electrically heated tubes. For the twin tube arrangements the tube pitch is varied between $s/d_F = 3.0$ and 1.05. The heat transfer on the upper tube of the twin tubes is enhanced compared with the single tube, while the heat transfer on the lower tube is not affected by the upper tube. The maximum heat transfer of the upper tube increases with increasing tube pitch.

1. INTRODUCTION

FINNED tubes are widely used to enhance heat transfer in refrigerants. A typical example is the tube bundle evaporator in refrigeration machinery.

In this investigation, a rudimentary arrangement of a tube bundle is chosen in order to learn about interrelated effects: starting with the heat transfer performance in boiling from a single finned tube—as a basis—a twin tube arrangement, with one tube above the other, is chosen as the simplest tube bundle.

Several studies concerning the boiling heat transfer on twin tube arrangements have been reported in refs. [1–4]. Most of these were performed for one tube pitch only. The effect of tube pitch has not yet been discussed.

This effect on the heat transfer characteristics is clarified by testing the twin tube arrangements with a varying tube pitch of $s/d_F = 3.0$; 1.3 and 1.05. Based on the experimental results a theory is proposed for the prediction of the heat transfer coefficients for single finned tubes and twin tube arrangements.

2. EXPERIMENTAL SET-UP

The experiments were performed in a stainless steel tank (length 680 mm; width 600 mm; height 370 mm) which was equipped with glass windows on three sides. The tank and the condenser were encased in a temperature controlled compartment. The test set-up is described in more detail in refs. [5, 6].

The refrigerant R11 ($CFCl_3$, monofluorotrichloromethane) was used at a pressure of $p_S = 1$ bar as a convenient test fluid with a boiling temperature of $\theta_S = 23.31°C$. The principal results found with this medium should not differ much from those for other fluids in a comparable state. A sketch of the tube arrangement is shown in Fig. 1.

The test tubes are made of copper with small fins ($h = 1.52$ mm). Two types of tubes are used: 19 fpi (19 fins per inch) and 26 fpi tubes. In Fig. 2 cross cuts and a description of the tubes are given. In order to determine the wall temperature, six NiCr–Ni thermocouples are inserted in bore holes of 0.55 mm width and different length.

The liquid and vapour temperature are measured respectively with three NiCr–Ni thermocouples. The tubes were heated electrically, the heating power is determined with a precision power meter of class 0.1. The vapour pressure is measured with a pressure gauge and a precision pressure sensor (both class 0.1).

3. EXPERIMENTAL PROCEDURE

The heat transfer coefficient for the finned tubes is defined by the equation

$$\alpha = \dot{Q}/[A(\theta_W - \theta_S)] \tag{1}$$

where $\dot{Q}$ is the measured heat flow, A the total surface area of the finned tube, θ_S the measured vapour temperature and θ_W the mean outside wall temperature as calculated from

$$\theta_W = (\Sigma\theta_i)/6 - \dot{Q} \ln (d_R/d_i)/(2\pi l\lambda_W). \tag{2}$$

Here θ_i is the temperature measured at six locations on the same diameter d_i, l the tube length and λ_W the thermal conductivity of copper.

For the diagrams, both a heat flux $\dot{q} = \dot{Q}/A$ and a heat duty per unit tube length $\dot{Q}/l$ were defined.

Before the experiments were performed, the test tubes were heated with the highest heating rate ($\dot{q} = 50\,000$ W m^{-2}) for at least 50 h in order to evade the starting effects and to obtain reproducible results. All experiments were run with the heat flux being decreased in steps from large to small values, so that hysteresis effects were avoided.

NOMENCLATURE

A	area
b	fin thickness
c_p	specific heat capacity
d	diameter
d_R	root diameter
f	frequency
g	gravitational acceleration
Gr	Grashof number
h	fin height
Δh_v	latent heat of evaporation
l	length
N	number of active nucleation sites
Nu	Nusselt number
p	pressure
Pr	Prandtl number
$\dot{Q}$	heat flow
$\dot{q}$	heat flux (heat flow density)
r	critical cavity radius
s	tube spacing
T	thermodynamic temperature
t	fin spacing
$\dot{V}$	volume flow density.

Greek symbols

α	heat transfer coefficient
β_0	contact angle
γ	coefficient of expansion
θ	temperature
$\Delta\theta$	temperature difference
$\Delta\theta^*$	superheat temperature difference
λ	thermal conductivity
ν	kinematic viscosity
ρ	density
σ	surface tension.

Subscripts

B	bubble
b	bottom segment
C	convection
cal	calculated
exp	experimental
F	finned tube
fC	free convection
FT	fin tip
i	inside
l	liquid
m	mean
mod	modified
S	saturation
s	side segment
SF	single finned tube
t	top segment
v	vapour
W	wall
1	lower tube
2	upper tube.

4. EXPERIMENTAL RESULTS

4.1. *Single finned tubes*

In Fig. 3 the heat transfer coefficients for single finned tubes are plotted versus the heat flux $\dot{q}$. The curve for a single plain tube (tube without fins) is presented for comparison.

For such a comparison these curves can essentially be divided into two sections according to the prevailing heat transfer regime:

(a) The free convection regime for $\dot{q} < 1000\ \mathrm{W\,m^{-2}}$ with heat transfer coefficients for the finned tubes being smaller than for the plain tube. This is maybe due to the boundary layers between the fins which can grow together at the fin base.

(b) The nucleate boiling regime for $\dot{q} > 1000\ \mathrm{W\,m^{-2}}$ where the heat transfer on the finned tubes is larger than on the plain tube. On finned tubes the effect of bubbles extends to a larger surface area, i.e. fin-flanks and fin-root, than for plain tubes. Moreover, in the fabrication process of fins more nuclei maybe created than with plain tubes. The heat transfer is better when the fins are closer together (26 fpi tubes). Observation shows a higher bubble density with the closer spaced fins. The $\Delta\theta$-net in Fig. 3 shows that the wall excess temperature θ_W is larger for the wider spaced fins.

4.2. *Twin tube arrangements*

Experimental results for two finned tubes arranged with three different tube pitches ($s/d_F = 3.0$, 1.3 and 1.05) are shown in Fig. 4. In order to show the effect of onflow to the upper tube, the ratio of the upper tube heat transfer coefficient α_{2F} to the single tube heat transfer coefficient α_{SF} is plotted versus the heat flux $\dot{q}$.

In the twin tube arrangements the heat transfer coefficient of the upper tube is in the boiling region ($\dot{q} > 1000\ \mathrm{W\,m^{-2}}$) always higher than that of a single tube. This is expected as the convective onflow of bubbles and liquid, rising from the lower tube, enhances the heat transfer on the upper tube. The heat transfer on the lower tube is not influenced by the upper tube.

For both fin spacings and all tube pitches, the curves are similarly bell shaped: with low values of $\alpha_{2F}/\alpha_{SF} \approx 1$ in the free convection region ($\dot{q} < 1000\ \mathrm{W\,m^{-2}}$), a maximum of $\alpha_{2F}/\alpha_{SF} \approx 2$ in the transition region ($1000 < \dot{q} < 10\,000\ \mathrm{W\,m^{-2}}$) between free convection and fully developed boiling and again values

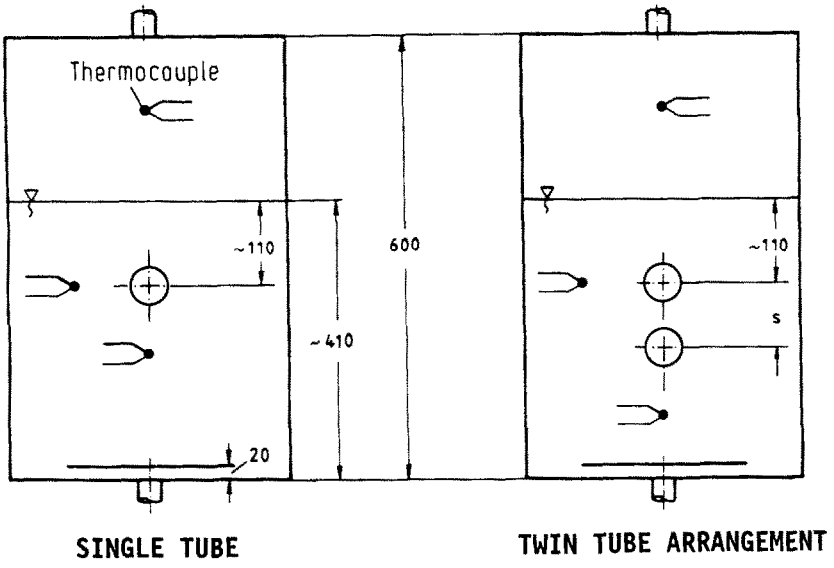

FIG. 1. Test tube arrangements.

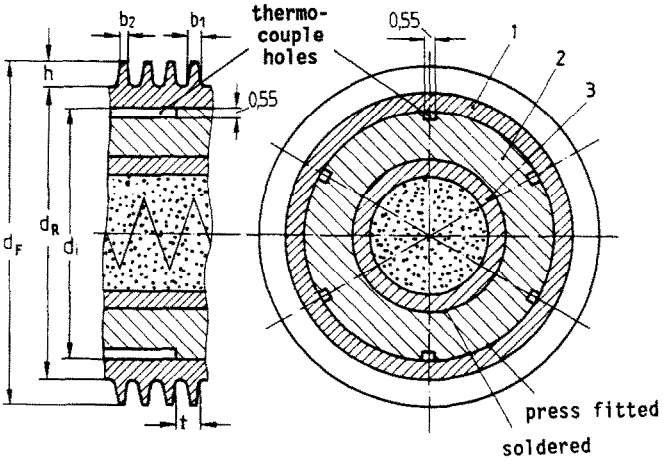

1. finned tube (copper)
2. filler tube (copper)
3. heating element

fins per inch	19	26
finned tube diameter d_F [mm]	18.74	18.89
root diameter d_R [mm]	15.70	15.85
fin height h [mm]	1.52	1.52
fin spacing t [mm]	1.30	1.03
fin thickness (base) b_1 [mm]	0.50	0.44
fin thickness (tip) b_2 [mm]	0.32	0.22
total surface area A [m^2/m]	0.1626	0.1952
area ratio A/A_R [-]	3.296	3.920

FIG. 2. Finned tube heater geometry.

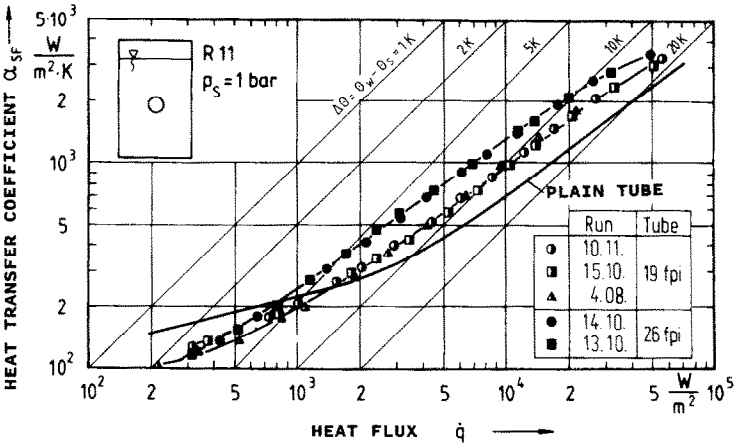

FIG. 3. Heat transfer coefficient (based on total surface area) on single finned tubes.

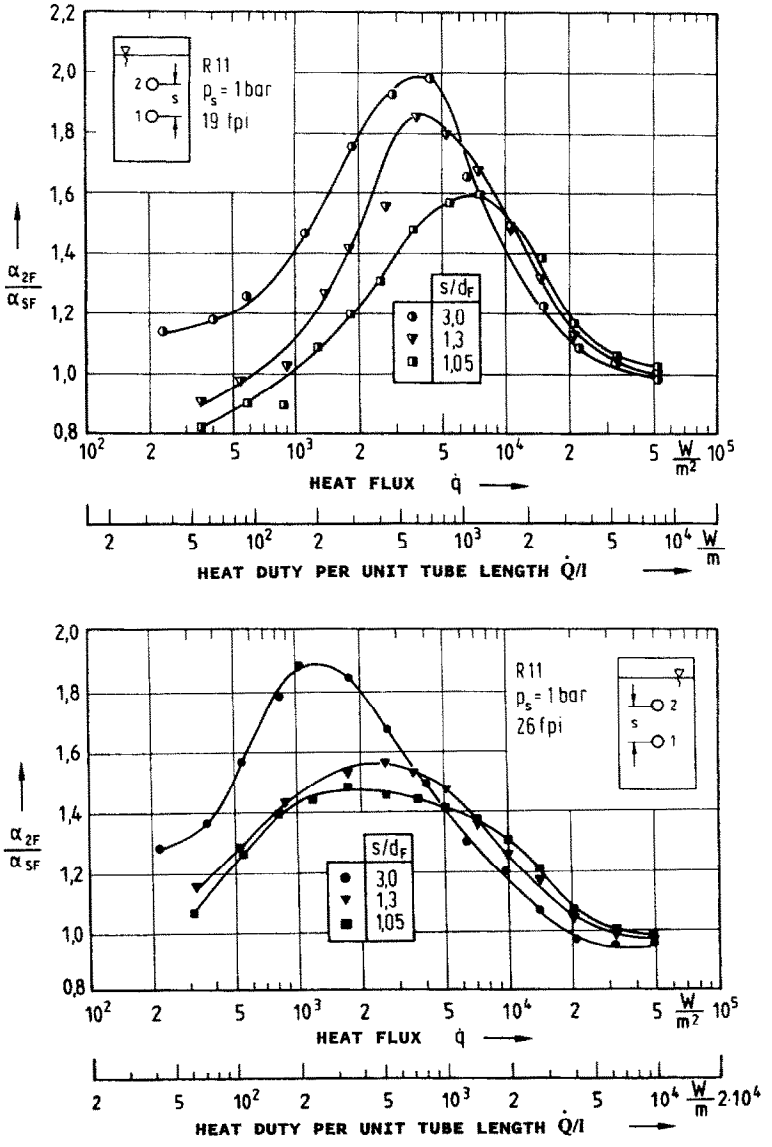

FIG. 4. Heat transfer coefficient of the upper finned tube, based on that of a single finned tube.

of $\alpha_{2F}/\alpha_{SF} = 1$ at fully developed nucleate boiling at 50 000 W m^{-2}. The wider spaced fins (19 fpi) give higher maximum values of α_{2F}/α_{SF} and higher values when boiling is approaching full development.

The highest values of $\alpha_{2F}/\alpha_{SF} \approx 2$ are obtained with a tube pitch of $s/d_F = 3.0$. The closest arranged tubes ($s/d_F = 1.05$) yield the smallest enhancement of the upper tube heat transfer with $\alpha_{2F}/\alpha_{SF} \approx 1.5$. At fully developed nucleate boiling neither fin spacing nor tube pitch exhibit any effect: the upper tubes behave just the same as a single tube so that $\alpha_{2F} \approx \alpha_{SF}$.

As usual in practical applications a scale for the heat transmitted per metre length of the finned tubes is also presented in Fig. 4.

5. THEORY

5.1. *Single finned tube*

Based on the theory of Mikic and Rohsenow [7] for plates and plain tubes, a theory is developed for finned tubes.

The transferred heat flux is divided into two parts: the heat flux transferred from the 'bubble influence area' due to nucleate boiling $\dot{q}_B$ and the heat flux transferred from the remaining surface due to convection $\dot{q}_C$

$$\dot{q} = \dot{q}_B + \dot{q}_C \tag{3}$$

with

$$\alpha = \dot{q}/(\theta_W - \theta_S). \tag{4}$$

(a) *Heat transfer from the bubble influence area*

Mikic and Rohsenow postulated an unsteady heat conduction from the heating wall into the adhering liquid. This mechanism is caused by the unsteady flow of liquid to the wall behind a departing bubble and it affects a so-called bubble influence area.

On finned tubes the bubbles grow chiefly at the fin-base, and rise along the fin-flanks. The superheated boundary layers in the fin-gaps are renewed between the successive processes of bubble departure and bubble growth. If an 'average liquid exchange frequency' f is applied for both the fin-flanks and the fin-base, the heat flux and the heat transfer coefficient in the bubble influence area is then calculated according to ref. [7] as

$$\dot{q}_B = \alpha_B(\theta_W - \theta_S)A_B/A \tag{5}$$

and

$$\alpha_B = 2(\lambda_l \rho_l c_{pl})^{1/2} f^{1/2} \pi^{-1/2}. \tag{6}$$

For plain tubes the influence area of a bubble is a circle of twice the bubble departure diameter d_B as proposed by Han and Griffith [8].

Thus, for N bubbles the area ratio is on plain tubes

$$\frac{A_B}{A} = \frac{N}{A}\frac{\pi}{4}(2d_B)^2. \tag{7}$$

For finned tubes the influence area of a bubble is assumed to be a band with the width of twice the bubble departure diameter d_B and an influential length l_i reaching across both fin-flanks and the fin-base.

Table 1. Empirical coefficients for the nucleation site density

Finned tube (fpi)	C (m^{-2})	r_0 (μm)	n
19	8.9294×10^{10}	14.973	0.2
26	2.7700×10^{10}	26.235	0.2

For N bubbles on a finned tube the area ratio is

$$\frac{A_B}{A} = \frac{N}{A} 2 d_B l_i \tag{8}$$

with

$$l_i = 2[(b_1 - b_2)^2/4 + h^2]^{1/2} + t - b_1$$

from a geometric consideration, and b_1 and b_2, etc. indicated in Fig. 2.

When an 'influence factor' F is introduced as

$$F = 2d_B l_i/[(2d_B)^2 \pi/4] \tag{9}$$

the area ratio in equation (8) becomes

$$\frac{A_B}{A} = \frac{N}{A}\frac{\pi}{4}(2d_B)^2 F. \tag{10}$$

The nucleation site density N/A can be obtained from a relation proposed by Salem [9]

$$\ln (N/A) = [1 - (r/r_0)^n] \cdot \ln C \tag{11}$$

where r is the critical radius of a bubble which can be calculated using Lord Kelvin's and Clausius–Clapeyron's equations

$$r = \frac{2\sigma T_S}{\Delta\theta \rho_v \Delta h_v}. \tag{12}$$

The empirical coefficients C, r_0 and n are obtained from the experimental results for the single finned tubes (see Table 1). The liquid exchange frequency f on finned tubes can be calculated similarly to that on plain tubes according to Knabe [10]:

When $A_B/A \leqslant 1 - A_{FT}/A$, with A_{FT} being the total area of the fin tips, the frequency f equals the bubble frequency

$$f = f_B. \tag{13}$$

When $A_B/A > 1 - A_{FT}/A$, the frequency is

$$f = f_B \cdot (A_B/A). \tag{14}$$

It is assumed that no bubbles grow on the area A_{FT}.

For an estimate of the bubble departure diameter, a relation proposed by Stephan [11] can be used

$$d_B = 0.851\beta_0\{2\sigma/[g(\rho_l - \rho_v)]\}^{1/2} \tag{15}$$

with the contact angle β_0 in radians.

The bubble frequency may be calculated with a relation presented by Zuber [12]

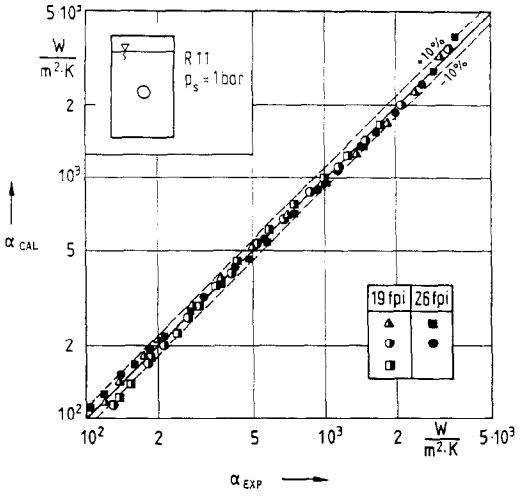

FIG. 5. Comparison between experimental and calculated heat transfer coefficients for single finned tubes.

$$f_B d_B = 0.59[\sigma g(\rho_l - \rho_v)/\rho_l^2]^{1/4}. \quad (16)$$

(b) *Heat transfer from the remaining surface*

The heat transfer mechanism in the remaining surface is free convection; the heat flux is given by

$$\dot{q}_C = \alpha_C(\theta_W - \theta_S)(1 - A_B/A). \quad (17)$$

For the finned tubes the heat transfer due to free convection can be calculated from a relation proposed by Kübler *et al.* [13]

$$Nu = -0.55 + 0.48(Gr_{mod}\, Pr)^{0.27} = \alpha_{fC}(t - b_2)/\lambda \quad (18)$$

with

$$Gr_{mod} = \frac{\gamma g(\theta_W - \theta_S)(t - b_2)^3}{\nu^2} \frac{t - b_2}{d_F} \quad (19)$$

and properties taken at $\theta_m = \theta_S + \Delta\theta/2$.

A comparison between calculated heat transfer coefficients and experimental ones is shown in Fig. 5. The calculated and measured values agree well. There is an average scatter for both types of finned tubes of 4.4%.

5.2. *Twin tube arrangements*

The heat transfer coefficient of the lower tube can be evaluated with the equations proposed for the single tube.

The heat flux of the upper tube again is divided into a boiling and a convection heat flux

$$\dot{q}_2 = \dot{q}_{B2} + \dot{q}_{C2} = \alpha_2(\theta_{W2} - \theta_S). \quad (20)$$

The convection heat flux is caused by the onflow of a liquid/vapour mixture.

(a) *Heat transfer from the bubble influence area*

The heat flux in the bubble influence area can be calculated according to equation (5)

$$\dot{q}_{B2} = \alpha_B(\theta_{W2} - \theta_S)(A_B/A)_2 \quad (5a)$$

with α_B from equation (6).

(b) *Heat transfer from the remaining surface*

Fujita *et al.* [4] developed a theory for twin plain tube arrangements. This is extended here to finned tubes.

Around the circumference of the upper tube the onflow of bubbles is nonuniform, so that the effect of convection varies with the position around the tube surface. Therefore, it appears logical to subdivide the circumferential area of the tube into bottom-, side- and top-segments, as in Fig. 6. We have

$$A = A_b + A_s + A_t \quad (21)$$

with a respective subdivision of heat fluxes

$$\dot{q}_{C2} = \dot{q}_{C2b} + \dot{q}_{C2s} + \dot{q}_{C2t}. \quad (22)$$

The bottom segment heat flux is

$$\dot{q}_{C2b} = \alpha_{C2b}\Delta\theta_2^*(A_b/A)[1 - (A_B/A)_2] \quad (23a)$$

the side segment heat flux is

$$\dot{q}_{C2s} = \alpha_{C2s}\Delta\theta_2^*(A_s/A)[1 - (A_B/A)_2] \quad (23b)$$

and the top segment heat flux is

$$\dot{q}_{C2t} = \alpha_{C2t}\Delta\theta_2^*(A_t/A)[1 - (A_B/A)_2] \quad (23c)$$

with

$$\Delta\theta_2^* = \Delta\theta_2 - \delta\theta_2.$$

The superheat excess temperature $\Delta\theta_2^*$ accounts for the superheat of the surrounding liquid $\delta\theta_2$ on the upper tube.

At the top segment of the upper tube, no influence of rising bubbles is assumed so that the heat transfer coefficient can be calculated from equation (18)

$$\alpha_{C2t} = \alpha_{fC}. \quad (24)$$

The side and bottom segments are affected by the rising bubbles and thus a relationship with the onflow

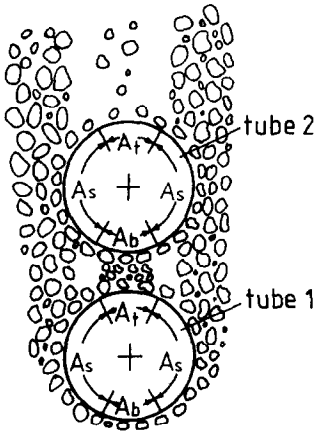

FIG. 6. Subdivision of the tube surface-area into bottom (A_b)-, side (A_s)- and top (A_t)-segments.

has to be introduced, e.g. in the following form for the bottom segment:

$$\alpha_{C2b} = \alpha_C(\dot{V}_{2b}) \tag{25}$$

where $\alpha_C(\dot{V}_{2b})$ is the convection heat transfer coefficient as a function of the vapour volume flow density. This volume flow density for the bottom segment can be obtained from

$$\dot{V}_{2b} = k\frac{A_t}{A}\frac{\dot{q}_{B1}}{\Delta h_v \rho_v} \tag{26}$$

where A_t is the top segment area of tube 1 which is equal to that of tube 2. The factor k is a constant which accounts for the fact that only part of the heat flux from the lower tube $\dot{q}_{B1}$ is consumed for bubble generation and another small part for superheating of the fluid.

The convection heat transfer coefficient at the side segments is introduced as

$$\alpha_{C2s} = \alpha_C(\dot{V}_{2s}). \tag{27}$$

The respective vapour volume flow density, according to ref. [4] is

$$\dot{V}_{2s} = \dot{V}_{2b} + k\left[\dot{q}_{C2b} + \frac{A_b}{A}\dot{q}_{B2} + \left[\frac{A_b}{A} + \frac{A_s}{A}\right]\dot{q}_{B1}\right]\frac{1}{\Delta h_v \rho_v} \tag{28}$$

with $\dot{q}_{B2}$ and $\dot{q}_{B1}$ as the boiling heat fluxes on the upper and lower tube.

The term $\dot{V}_{2b}$ in equation (28), equals the vapour flow $\dot{V}_{1t}$ from the top segment of the lower tube which hits the bottom segment of the upper tube. The heat flux $\dot{q}_{C2b}$ originating in the bottom segment of the upper tube, causes partial evaporation of the thin boundary layer and thus another vapour flow. The term $(A_b\dot{q}_{B2})/A$ gives the contribution from the bubbles generated on the bottom segment of the upper tube; finally, the fourth term represents the contribution of bubbles formed at the bottom and side segments of the lower tube.

The area ratios in equations (23), (26) and (28) are estimates, determined by direct observation. They are listed in Table 2 for the various tube pitches.

The convective heat transfer on the upper tube consists of a free convection part and an onflow part depending on the vapour flow density. Accordingly a relation of the form

Table 2. Area ratios

Tube pitch, s/d_F	A_b/A	A_s/A	A_t/A
3.0	0	0.9	0.1
1.3	0.1	0.8	0.1
1.05	0.15	0.7	0.15

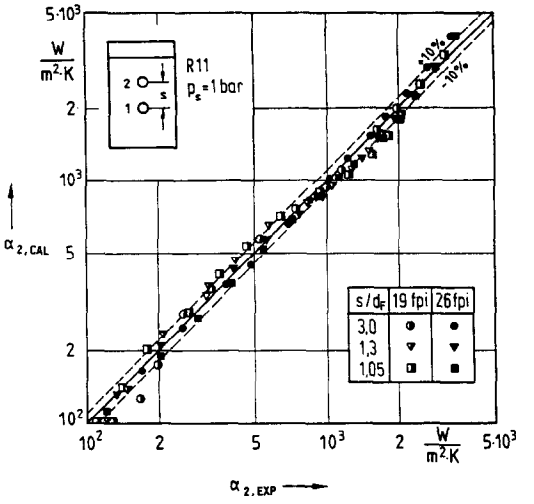

FIG. 7. Comparison between experimental and calculated heat transfer coefficients for the upper tube of twin finned tubes.

$$\alpha_C(\dot{V}) = \alpha_{fC} + \alpha_0(\dot{V}) \tag{29}$$

is considered.

From the experimental results for the twin tube arrangements with tube pitch $s/d_F = 3.0$ the following function $\alpha_0(\dot{V})$ was determined

$$\alpha_0(\dot{V}) = \alpha_0 \exp\left(-[\dot{V}_0/(\dot{V}/k)]^m\right) \tag{30}$$

with $\alpha_0 = 1750$ W m^{-2} K^{-1}, $\dot{V}_0 = 1.439 \times 10^{-3}$ m s^{-1} and $m = 0.462$ so that equation (29) becomes

$$\alpha_C(\dot{V}) = \alpha_{fC} + 1750 \exp\left(-[1.439 \times 10^{-3}/(\dot{V}/k)]^{0.462}\right). \tag{31}$$

The heat transfer coefficients α_{C2b} and α_{C2s} can be calculated from equation (31) when the respective $\dot{V}/k$ from equations (26) and (28) is inserted.

The constant k does not need to be determined when it is used in the form $\dot{V}/k$.

The liquid superheat, necessary for the calculation of $\dot{q}_{C2b}$, etc. [equation (23a) ff.] was measured on the unheated upper tube (using its thermocouples) with the lower tube heated with specified heat fluxes. The superheat $\delta\theta_2$ varies from 0 to 2 K. For more details see ref. [14].

In Fig. 7 comparison is made for the heat transfer coefficient α_2 as obtained from the experiment or the calculation. The heat transfer coefficient α_2 is defined in equation (20). The average deviation between measured and calculated values amounts to 7.7%.

Although only the results for $s/d_F = 3.0$ were used for the determination of the coefficients in equation (31), this equation seems good enough to fit data for the other tube pitches. Thus the effect of tube pitch on the heat transfer is well accounted for by the introduction of area ratios respective to tube pitch. The side segment has the highest heat transfer coefficients due to the enhanced convection, and it gives the maximum effect on the heat transfer. It seems appro-

priate that the area ratio of the side segment is assumed to increase with increasing tube pitch. Consequently, the heat transfer from the upper tube in twin tube arrangements also increases with increasing tube pitch in accordance with experimental results.

6. SUMMARY

Single finned tubes exhibit smaller heat transfer coefficients than plain tubes in the free convection heat transfer regime ($\dot{q} < 1000$ W m^{-2}). In the nucleate boiling regime, however, the heat transfer coefficient from single finned tubes exceeds that of plain tubes. The heat transfer coefficient from 26 fpi tubes is better than that from 19 fpi tubes.

For twin finned tube arrangements in pool boiling the heat transfer coefficient of the upper tube is higher than that of the lower tube, which is equal to that of the single tube. The enhancement in heat transfer is largest in the transition region between nucleate boiling and free convection, it vanishes at high and low heat fluxes. For bottom (lower) tubes the heat transfer on 26 fpi tubes is better than that on 19 fpi tubes, but for the upper tubes, which are in the wake of the lower tubes, the opposite results were obtained. Large pitches ($s/d_F = 3.0$) give higher heat transfer coefficients than small pitches ($s/d_F = 1.05$) as long as fully developed boiling is not reached. At fully developed boiling neither tube pitch nor fin spacing shows any effect on the heat transfer coefficient.

Based on the theory proposed by Mikic and Rohsenow for plain tubes, a theory is developed for finned tubes. The new theory considers bubble dynamics and interaction between the heat transfer mechanisms of boiling and natural convection, as well as the effect of the fin geometry. Calculated and measured values agree well.

For the twin tube arrangements the theory of Fujita for plain tubes is extended to finned tubes. The tube pitch effect is well reproduced by the theory. The calculated results are in good agreement with the experimental results.

Acknowledgement—This investigation was carried out with the support of the Deutsche Forschungsgemeinschaft. The authors gratefully acknowledge this. The authors are also indebted to Wieland-Werke AG, Ulm, who provided the finned tubes for experiments.

REFERENCES

1. M. Güttinger, Die Verbesserung des Wärmeübergangs bei der Verdampfung in überfluteten Rohrbündelverdampfern, *Proc. 4th IHTC*, Paper HE2.4 (1970).
2. E. Hahne, Pool boiling and the effect of pool geometry, *Wärme- und Stoffübertr.* **17**, 155–159 (1983).
3. F. Zimmermann, Messung der Wärmeübergangskoeffizienten von verdampfenden Kältemitteln bei überfluteter Verdampfung, *Klima-Kälte-Heizung* **10**, 430–436 (1982).
4. Y. Fujita, H. Ohta, S. Hidaka and K. Nishikawa, Nucleate boiling heat transfer on horizontal tubes in bundles, *Proc. 8th IHTC*, San Francisco, pp. 2131–2136 (1986).
5. E. Hahne and J. Müller, Boiling on a finned tube and a finned tube bundle, *Int. J. Heat Mass Transfer* **26**, 849–859 (1983).
6. J. Müller, Boiling heat transfer on finned tube bundles—the effect of tube position and intertube spacing, *Proc. 8th IHTC*, San Francisco, pp. 2111–2116 (1986).
7. B. B. Mikic and W. M. Rohsenow, A new correlation of pool-boiling data including the effect of heating surface characteristics, *J. Heat Transfer* **91**, 245–250 (1969).
8. C.-Y. Han and P. Griffith, The mechanism of heat transfer in nucleate pool boiling, Parts I and II, *Int. J. Heat Mass Transfer* **8**, 887–914 (1965).
9. M. I. Salem, Wärmeübergang beim Blasensieden und Größenverteilung von stabilen Blasenkeimen sowie von Rauhigkeitsvertiefungen der Heizfläche, Diss. Universität Karlsruhe (1979).
10. V. Knabe, Zum Einfluß der Heizflächenrauhigkeit auf den Wärmeübergang und die maximale Wärmestromdichte beim Blasensieden, Diss. Universität, Paderborn (1983).
11. K. Stephan, *Wärmeübergang beim Kondensieren und beim Sieden*. Springer, Berlin (1988).
12. N. Zuber, Hydrodynamic aspects of boiling heat transfer, U.S. AEC Rep., AECU 4439 (1959).
13. R. Kübler, M. Bierer and E. Hahne, Heat transfer from finned and smooth tube heat exchanger coils in hot water stores, ISES Solar World Congress, Hamburg (1987).
14. R. Windisch, Wärmeübergang beim Sieden von Kältemittel an Einzelrohren, Zweirohranordnungen und Rohrbündeln, *DKV Forschungsbericht* **26** (1989).

TRANSFERT THERMIQUE PAR EBULLITION EN RESERVOIR SUR DES TUBES AILETES—ETUDE THEORIQUE ET EXPERIMENTALE

Résumé—Le transfert thermique par ébullition en réservoir de R11 est étudié expérimentalement et théoriquement sur des tubes uniques et deux arrangements de tubes jumeaux. On utilise des tubes ailetés avec 19 et 26 ailettes par inch. Le refrigérant s'évapore à l'état de saturation de 1 bar sur l'extérieur des tubes chauffés électriquement. Pour les arrangements de tubes jumeaux, le pas entre tubes varie entre $s/d_F = 3{,}0$ et 1,05. Le transfert thermique sur le tube supérieur est augmenté, comparé au cas d'un tube unique, tandis que le transfert thermique sur le tube inférieur n'est pas affecté par le tube supérieur. Le transfert de chaleur maximal sur le tube supérieur croît avec l'augmentation du pas entre tubes.

WÄRMEÜBERGANG BEIM BEHÄLTERSIEDEN AN RIPPENROHREN—EINE EXPERIMENTELLE UND THEORETISCHE UNTERSUCHUNG

Zusammenfassung—Der Wärmeübergang beim Behältersieden von R11 an Einzelrohren und Zweirohranordnungen wird experimentell und theoretisch untersucht. Dabei werden Rippenrohre mit 19 und 26 fpi (Rippen je Zoll) verwendet. Das Kältemittel verdampft beim Sättigungsdruck von 1 bar an der Außenseite der elektrisch beheizten Rohre. Für die Zweirohranordnung wird das Teilungsverhältnis zwischen $s/d_F = 3{,}0$ und 1,05 variiert. Der Wärmeübergang am oberen Rohr der Zweirohranordnungen verbessert sich gegenüber dem Einzelrohr, während der Wärmeübergang am unteren Rohr nicht vom oberen Rohr beeinflußt wird. Der maximale Wärmeübergang am oberen Rohr nimmt mit wachsendem Teilungsverhältnis zu.

ТЕПЛОПЕРЕНОС НА ОРЕБРЕННЫХ ТРУБАХ ПРИ КИПЕНИИ В БОЛЬШОМ ОБЪЕМЕ. ЭКСПЕРИМЕНТАЛЬНОЕ И ТЕОРЕТИЧЕСКОЕ ИССЛЕДОВАНИЕ

Аннотация—Экспериментально и теоретически исследуется теплоперенос при кипении R11 на единичных трубах или в системах парных труб. Используются оребренные трубы с 19 и 26 ребрами на дюйм. Хладагент испаряется, когда давление насыщения на наружной стороне труб, нагреваемых электрическим током, составляет 1 бар. В случае систем парных труб шаг между ними изменяется от $s/d_F = 3{,}0$ до 1,05. На верхней из парных труб теплоперенос является более интенсивными, чем на единичной трубе, в то время как на нижней трубе он не зависит от наличия верхней. Максимальный коэффициент теплообмена на верхней трубе увеличивается с ростом шага между трубами.